

**GT2011-453- -**

## **STIFFNESS MEASUREMENT FOR PRESSURE-LOADED BRUSH SEALS**

**Rahul A. Bidkar**

General Electric - Global Research Center  
Niskayuna, NY, 12309 USA

**Mehmet Demiroglu**

General Electric - Energy & Infrastructure  
Schenectady, NY, 12345 USA

**Xiaoqing Zheng**

General Electric - Energy & Infrastructure  
Schenectady, NY, 12345 USA

**Norman Turnquist\***

General Electric - Global Research Center  
Niskayuna, NY, 12309 USA

\*Corresponding Email: turnquist@ge.com

### **ABSTRACT**

Brush seals are widely used as flexible seals for rotor-stator and stator-stator gaps in power generation turbo-machinery like steam turbines, gas turbines, generators and aircraft engines. Understanding the force interactions between a brush seal bristle pack and the rotor is important for avoiding overheating and rotor dynamic instabilities caused by excessive brush seal forces. Brush seal stiffness (i.e. brush seal force per unit circumferential length per unit incursion of the rotor) is usually measured and characterized at atmospheric pressure conditions. However, the inter-bristle forces, the blow-down forces and the friction forces between the backplate and the bristle pack change in the presence of a pressure loading, thereby changing the stiffness of the brush seal in the presence of this pressure loading. Furthermore, brush seals exhibit different hysteresis behavior under different pressure loading conditions. Understanding the increased brush seal stiffness and the increased hysteresis behavior of brush seals in the presence of a pressure loading is important for designing brush seals for higher pressure applications. In this article, we present the development of a test fixture for measuring the stiffness of brush seals subjected to a pressure loading. The fixture allows for measurement of the bristle pack forces in the presence of a pressure loading on the seal while the rotor is incrementally pushed (radially) into the bristle pack. Following the development of this test fixture, we present representative test results on three sample seals to show the trends in brush seal stiffness as the pressure loading is increased. Specifically, we study the effect of different brush seal design parameters on the stiffness of brush seals over a wide range of pressure loadings. These test data can be used for developing predictive models for brush seal stiffness under pressure loading.

Furthermore, we demonstrate the utility of this fixture in studying the hysteresis exhibited by brush seals along with the importance of the backplate pressure balance feature present in several brush seal designs. The test results validate the bi-linear force-displacement curves previously reported in the literature.

### **1.0 INTRODUCTION**

Brush seals are used in gas turbines, steam turbines and aircraft engines for sealing a wide range of stator-stator and rotor-stator gaps [1,2]. A typical brush seal (See Figure 1) consists of a flexible bristle pack welded to the side plate at the outer diameter. This bristle pack is held between a front plate and a backplate. The front plate protects the bristle pack from upstream disturbances while the backplate is primarily present to support the bristle pack against pressure loads. For rotor-stator gaps undergoing a radial transient, flexible brush seals are clearly a better choice [2] over labyrinth seals, which need a large steady state clearance (and thereby a compromised leakage performance) to avoid rubbing during the radial transient. Several experimental [2,3,4] and numerical studies [5,6] have investigated the effects of seal geometry (bristle pack density, bristle diameter, bristle material, cantilever angle, fence height, backplate designs) on key performance characteristics of brush seals like leakage, pressure capability, stiffness, seal wear and seal life [2]. Two key performance characteristics of brush seals are stiffness and hysteresis behavior. Stiffness of a brush seal is a measure of the force interactions between the bristle pack and the rotor. Brush seal stiffness has direct implications for thermally induced rotor dynamic instabilities [7,8], seal wear and seal life. Brush seal

hysteresis is a measure of the ability of the seal to recover and follow the rotor as the rotor retracts after a radial incursion. Seal hysteresis has a direct impact on the ability of the seal to maintain small operating clearance (and thereby small leakage) after a rotor incursion. Seal stiffness and seal hysteresis increase with increasing pressure load across the brush seal, thereby limiting the use of these seals at high-pressure loads [9,10]. Brush seal designers have to rely on limited experimental data at high pressure for designing brush seals at high-pressure loads. In order to improve the applicability of brush seals at high-pressure loads, it is necessary to characterize and reduce seal stiffness and seal hysteresis at high-pressure loads. In this study, we develop a test fixture and demonstrate it for characterizing brush seal stiffness and hysteresis in the presence of a pressure loading on the brush seal.

Brush seal stiffness is defined as the radial force per unit circumferential seal length of the seal that is needed to radially displace the bristles by unit magnitude. Seal stiffness at *atmospheric pressure conditions* can be explained using simple beam models [11,12] for the bristle or complex finite element models that model bristle-to-bristle interactions [13], with the latter agreeing better with seal stiffness test data at atmospheric pressure conditions. Seal stiffness increases significantly in the presence of a pressure load. With increasing pressure load, the bristle pack gets pushed against the back plate. The resulting increased normal reaction leads to an increased frictional force between the bristles and the back plate (See Figure 1). This increased frictional force opposes the radial movement of the bristle pack, thereby causing stiffening of the bristle pack along with seal hysteresis. There are limited experimental data [9,10,12,14] and some modeling attempts [15] for understanding brush seal stiffening and increased hysteresis under a pressure load. Specifically, Basu et al. [9] and Aksoy and Aksit [10] use small-radius circular brush seals (under pressure) arranged around a stationary/rotating rotor disk to directly measure bristle-rotor forces for varied degrees of rotor interference. Brush seal stiffness under pressure loading is indirectly estimated in the work of Demiroglu and Tichy [12] and Wood and Jones [14] through the measurements of changing torque on a rotor which runs with interference with pressure loaded circular brush seals. In this article, we develop a test fixture for measuring brush seal stiffness for large-diameter brush seals. In order to test large diameter brush seals, we would need a large rotating rig, which can become relatively cumbersome during testing. As a consequence, we restrict our testing to a stationary rotor, where only a segment of the rotor interferes with the brush seal bristle pack. Thus, the test data presented in this article are for large-diameter brush seals with an interfering stationary rotor, as against the test data for small-diameter brush seals obtained using an interfering rotating rotor [9,10,14].

The remaining portions of this article are arranged in the

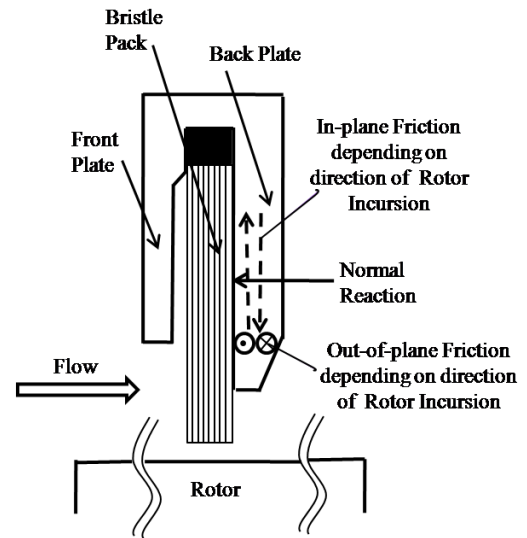


**Figure 1: Brush seal cross-section showing normal reaction and friction force between the bristle pack and the back plate.**

following fashion. In section 2, we summarize the design features of the stiffness-measuring test fixture, list the instrumentation used during testing and briefly describe the test procedure. In section 3, we present data analysis procedures. In section 4, we present test data for three different brush seal samples, with force-displacement curves and hysteresis data for seal sample 1 and seal sample 3, and brush seal stiffness variation with pressure for seal sample 1 and seal sample 2. Finally, in section 5, we present conclusions from this work.

## 2.0 STIFFNESS MEASURING TEST FIXTURE

The test fixture is intended for measuring the stiffness of brush seals when they are subjected to a pressure loading in a high-pressure chamber test rig at General Electric Global Research Center. This section describes the working principle of the fixture.

A three-dimensional representation of the test fixture is shown in Figure 2 while a detailed cross-section of this fixture is shown in Figure 3. The fixture consists of two large-diameter brush seals mounted on a circular seal support. The brush seal mounted on the right side is the test seal and is fixed to the circular seal support. The large-diameter rotor is simulated with a rectangular block with the rotor radius machined on either side (see rotor carrier in Figure 2 and 3). The rotor is mounted on a low-friction slide and can move along the X-direction radially relative to the test seal. The dummy brush seal on the left side is not fixed and can slide on the circular seal support along the X-direction. The dummy seal is pulled in the positive X-direction with hooks attached to the carrier rotor, and pushed in the negative X-direction with

spacer pins (not seen in Figure 2 and 3) such that the dummy seal bristles always remain line-on-line contact with the rotor. High-pressure air surrounds the entire fixture and low-pressure air is present inside the circular seal support, thereby creating a pressure drop across the bristles. The radial motion of the rotor relative to the brush seal is measured with two displacement sensors mounted on either side of the rotor. The force exerted by the bristle pack on the rotor is measured with a multi-axis load cell mounted between the rotor and the hydraulic actuator. This test fixture has several features that allow for accurate measurement of the bristle forces on the rotor. These features are briefly described below in subsections 2.1, 2.2 and 2.3.

### 2.1 THE SHOE & THE ROTOR

The purpose of the shoe is to reduce the end effects. When a finite-extent shoe pushes into the bristle pack, it tends to open or separate the bristle pack on one end because of the cantilever angle of the bristle pack (see Figure 4). This can lead to inaccurate measurement of bristle forces. In order to address this issue, both the rotor and the shoe push into the bristle pack, but only the forces exerted on the shoe are measured with the load cell. The rotor ensures that the bristle pack does not separate at one end, thereby reducing the end effects. Note that the shoe can move relative to the rotor. The small gap between the shoe and the rotor is sealed with an O-ring to block air jets emanating from the high-pressure side on

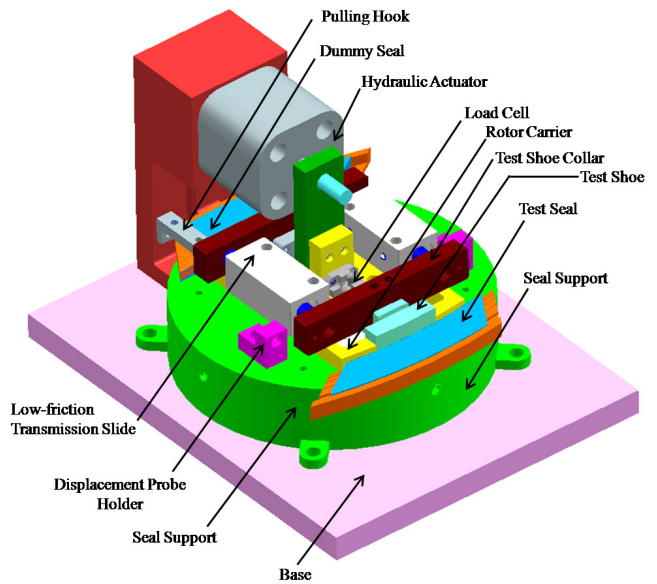


**Figure 2: Stiffness measurement test fixture showing the test seal and the dummy seal mounted on either side of a rotor.**

to the bristle pack. The force between the O-ring and the shoe interferes with the load cell measurements. However, the relative motion between the shoe and rotor is very small (of the order of microns because of a very stiff load cell). As a

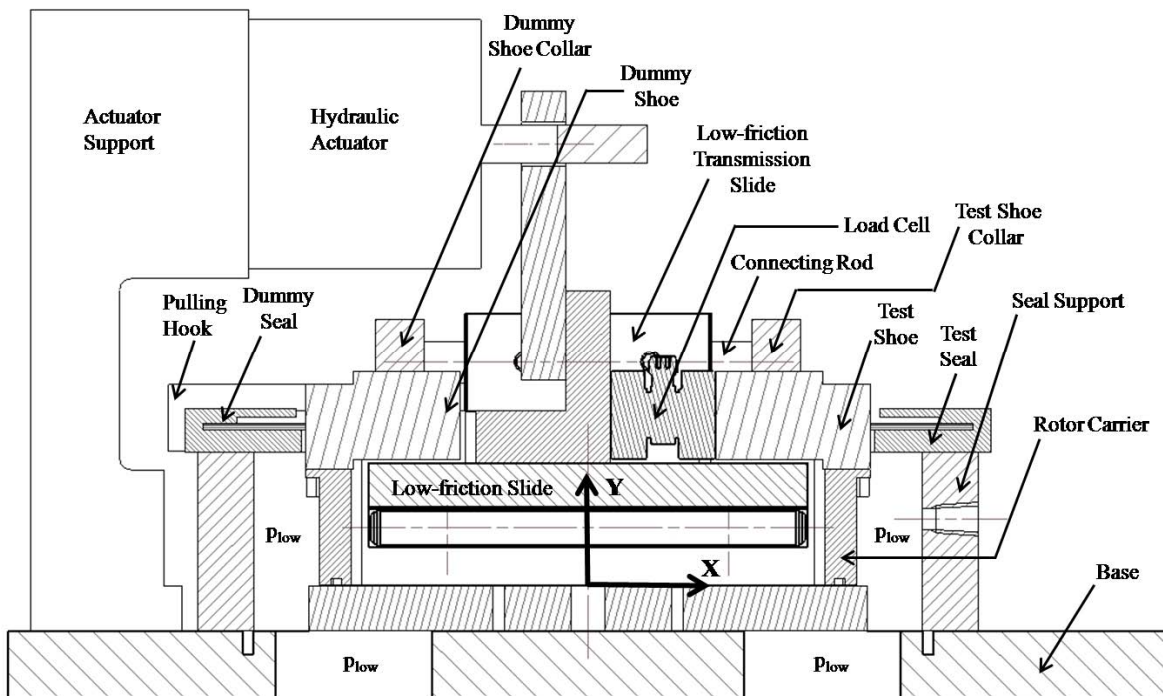


**Figure 3: Cross-section view of the Stiffness Testing Fixture**

consequence, the force caused by squeezing or deforming the O-ring is expected to be very small and its effect on the measurement is neglected.

## 2.2 DUMMY BRUSH SEAL

The purpose of the dummy brush seal is to counter-balance the *initial* air film pressure<sup>1</sup> between the test seal and the rotor and the *initial* blow-down forces<sup>2</sup> acting on the rotor. As the rotor is pushed into the test seal, the air film pressures and the blow-down forces change from their initial values. These changes are part of the brush seal stiffness and need to be recorded by the load cell. However, the initial air film pressures and the initial blow-down forces are not part of the stiffness measurement and need to be subtracted from the measurement. The dummy brush seal along with an assembly of the dummy shoe, connecting rods and low-friction slides are used to create the counter-balancing force. This assembly is described in the next subsection.

## 2.3 CONNECTING RODS & TRANSMISSION SLIDES ASSEMBLY

The counter-balancing force created by the dummy brush seal is transmitted to the load cell using an assembly of the dummy shoe, shoe collars, connecting rods and low-friction transmission slides. In order to understand the role played by this assembly in transmitting the counter-balancing force, it is important to understand the kinematics of the various moving parts of the test fixture.

As shown in Figure 3, the rotor carrier (mounted on the low-friction slide) can slide along the X-direction relative to the fixed base, fixed seal support and the fixed test seal. Two low-friction transmission slides are attached to the moving rotor carrier. These low-friction transmission slides support two connecting rods, which support the two shoe collars attached to the dummy shoe on the left and the test shoe on the right. The dummy shoe, the dummy shoe collar, the two connecting rods, the test shoe collar and the test shoe can thus move as one rigid assembly (supported by the low-friction transmission slides) along the X-direction relative to the rotor carrier. The test shoe is directly connected to the load cell

<sup>1</sup> For line-on-line assembly, the pressure of the air film between the rotor and the bristle pack varies linearly from  $P_{high}$  to  $P_{low}$  as we travel from the first bristle upstream of the bristle pack to the last bristle downstream of the bristle pack along the axial direction. This pressure of the air film exerts an initial force on the rotor. As the rotor is pushed into the test seal, this linear pressure drop from  $P_{high}$  to  $P_{low}$  might change to some other pressure drop distribution from  $P_{high}$  to  $P_{low}$  resulting in a changed force on the rotor. This changed force is part of the brush seal stiffness and needs to be recorded by the load cell. However, the initial force caused by this pressure is not part of the seal stiffness and needs to be cancelled/counter-balanced.

<sup>2</sup> For line-on-line assembly and a given pressure loading, the bristles blow down on the rotor and exert a force on the rotor. This is the initial blow-down force. As the rotor is pushed into the test seal, the blow-down force changes from its initial value and this change needs to be recorded by the load cell. Since the initial blow-down force is not part of the stiffness measurement, it needs to be cancelled/counter-balanced.

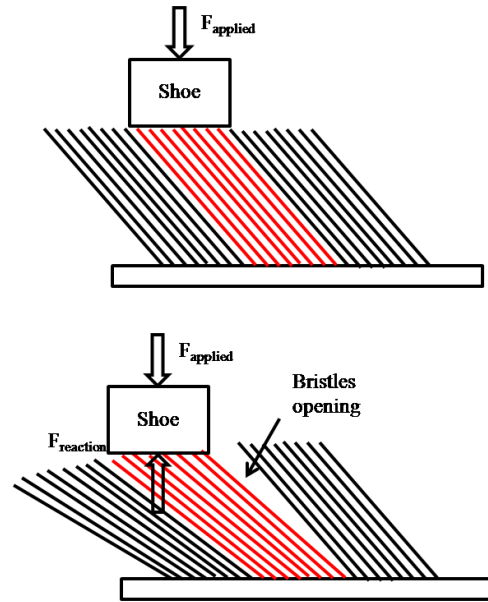


**Figure 4: Bristle opening caused by using a finite-extent shoe.**

while the dummy shoe is connected to the test shoe through the assembly described above. Thus, bristle pack forces from the test seal (acting from right to left) will compress the load cell. However, the bristle pack forces from the dummy seal (acting from left to right) that get transmitted through the connecting rods, pull the load cell and thus provide a counter-balancing force. Note that the dummy shoe and the test shoe are assembled in the same X-Z plane, and as long as the test seal and the dummy seal are identical (i.e. have bristles located in the same X-Z plane), the counter-balancing and cancellation of initial forces will occur without any resultant moments. Care needs to be exercised to ensure that bristles from both the test seal and the dummy seal lie approximately in the same X-Z plane as the load cell. With this fixture, testing is restricted to brush seals sets with approximately similar axial thicknesses. Testing seals with thickness vastly different from the samples tested in this work, requires a reduction/increase in the height (y-dimension) of the circular seal support.

During testing, both the test seal and the dummy seal are assembled line-on-line on either side of the rotor carrier. For a given pressure loading, both seals exert an initial air film pressure and an initial blow-down force on the rotor. However, since the dummy shoe is connected to the test shoe as described above, the net force recorded by the load cell is zero. Now, as we push the rotor carrier into the test seal, the air film and blow-down forces change for the test seal, but they remain unchanged for the dummy seal because the dummy brush seal moves along with the rotor (always maintaining the line-on-line contact) and always produces the same counterbalancing force. The load cell records only the change in the air film

pressure and the change in the blow-down forces along with the bristle pack resistance to deformation. Note that during testing, the dummy brush seal is pulled with hooks (see Figure 2 and 3) to move along with the rotor. The gap between the rotor and the dummy brush seal is always maintained constant with spacer pins (not seen in Figure 2 and 3) oriented along the direction of motion mounted on the rotor carrier.

## 2.4 TEST PROCEDURE

The test fixture is placed in a high-pressure chamber test rig at General Electric Global Research Center. The test brush seal is fixed on the seal support and located accurately using dowel pins. The rotor carrier is moved until it reaches line-on-line contact with the test brush seal. The dummy brush seal is mounted in the opposite end. The line-on-line zero clearance between the dummy seal and the rotor is maintained using spacer pins on the vertical face of the rotor carrier. Two hooks are mounted on the rotor carrier that engage with the dummy seal. The hooks ensure that the dummy seal is pulled forward when the rotor carrier moves forward into the test brush seal. The spacer pins on the vertical face of the rotor ensure that the dummy seal gets pushed backwards when the rotor carrier moves backwards. The displacement sensors are assembled after both brush seals are assembled line-on-line with the rotor.

After finalizing the assembly, the first thing is to perform the no-airflow test. With no air flowing through the rig, the rotor carrier is moved backwards so that there is a clearance between the rotor carrier and the test brush seal. Note that the dummy brush seal is still line-on-line contact. The rotor carrier is now slowly incremented forward to create interference between the rotor and the test brush seal. Throughout this procedure, the load cell data and the displacement sensor data are acquired at a pre-decided rate of 10 Hz. The procedure with flowing air is identical except we now log data from the pressure sensors as well. Special care needs to be taken while incrementing the rotor because a large actuation effort is needed at higher pressures due to friction between various moving parts. Note that these increased friction forces do not interfere with the actual measurement of seal stiffness.

## 3.0 DATA ANALYSIS PROCEDURE

The output of the load cell (volts) is multiplied by the calibration constant to obtain the force in units of pounds (or equivalently newtons). Furthermore, this force is divided by the circumferential length of the shoe to obtain the force exerted per unit circumferential length of the bristle pack. Note that the load cell output (volts) depends on the surrounding pressure in the high-pressure chamber. This dependence of the load cell output on the surrounding pressure is recorded for different surrounding pressures, and the correct bristle pack force is obtained by subtracting this recorded value from all test data.

The radial displacement of the rotor relative to the bristle pack is obtained by taking the arithmetic mean of the two

readings of the displacement sensors mounted on either side of the rotor. Finally, stiffness of the bristle pack is obtained by calculating the slope of the force per unit circumferential length (lb/inches or equivalently newton/meter) versus rotor displacement (inches or equivalently meter) curves. Thus, the unit for stiffness of the brush seals in this work is pounds/inch/inch (psi) (or equivalently newton/meter/meter (Pa)). Note, that there exists another method [11], which calculates the bristle tip pressure per unit displacement of the rotor i.e. psi/inch or equivalently Pa/meter. While, the seal stiffness presented in the present work is a direct measure of the radial force interaction (per unit circumferential length) between the rotor and the brush seal, the latter quantity allows us to directly compare brush seals with different bristle diameters.

## 4.0 HYSTERESIS AND STIFFNESS DATA

In this article, we present test data for three different brush seal samples, with force-displacement curves and hysteresis data for seal sample 1 and seal sample 3, and brush seal stiffness variation with pressure for seal sample 1 and seal sample 2. These three brush seal samples differ from one another in terms of brush seal geometry (bristle length, cantilever angle and bristle diameter). Apart from this, these three samples have different back plate designs intended for reducing pressure stiffening and brush seal hysteresis.

In Figure 5, we show the non-dimensional force per unit circumferential length for seal sample 1 as a function of displacement of the bristle pack. The four different curves correspond to different pressure loadings across the brush seal. We have normalized the force data in Figure 5 by the force  $F_0$ .  $F_0$  is the maximum force measured during the zero pressure loading case (i.e. the force measured at the maximum incursion of approximately 35 mils (0.889 mm) under atmospheric pressure conditions). The zero on the X-axis in Figure 5 represents the line-on-line assembly case for the test seal. The bottom X-axis represents displacement measured in mils (inch/1000) while the top X-axis is displacement in millimeters. Test data are collected starting with 10 mils (0.254 mm) clearance between the test seal and the rotor, while the dummy seal is line-on-line contact with the rotor throughout the test. As we push the rotor towards the test brush seal, the force increases. This trend continues until the maximum displacement. When the travel direction of the rotor is reversed, the load cell records a sudden drop in the measured force as seen in Figure 5. As we retract the rotor, the force reduces gradually but does not match exactly with the starting force at 10 mils (0.254 mm) clearance. There are two sources for this mismatch between the starting and ending force for a particular test cycle: (a) brush seal hysteresis (the primary quantity we want from this test rig apart from the stiffness), and (b) hysteresis caused by friction in the slides transmitting the dummy seal forces to the load cell. Both these sources of hysteresis are dependent on the pressure loading on

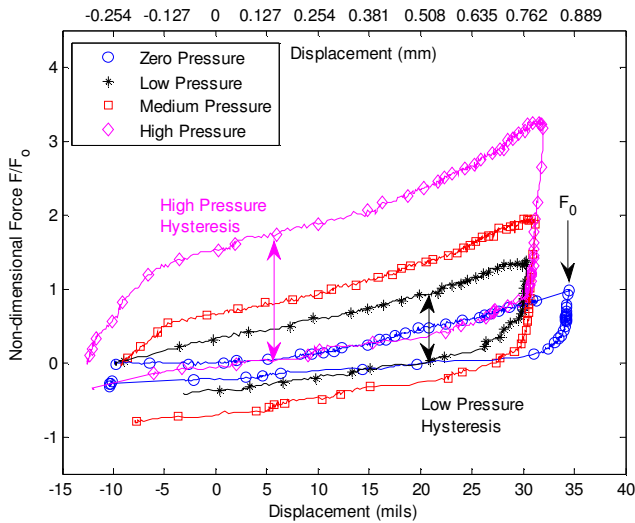


**Figure 5: Non-dimensional force as a function of bristle pack displacement for different pressure loadings across the brush seal sample 1.**

the stiffness rig, and an accurate estimate of the portion caused just by the brush seal hysteresis is not available. Quantifying the rig hysteresis portion out of the overall hysteresis is beyond the scope of the work presented in this article. However, we can argue that when comparing two different brush seal samples with identical pressure loading, the rig friction effects remain identical, while the brush seal hysteresis changes because of seal geometry. Thus comparing test results for two seals under identical pressure loading, we can investigate them for hysteresis performance.

The four different curves shown in Figure 5 although shown to start with a zero force at the beginning of their corresponding test cycle, do not actually start with zero force at 10 mils (0.254 mm) clearance (between the test seal and the rotor). It should be noted that after the zero-pressure loading test, when the system is pressurized, there are blow-down forces from the dummy seal and friction forces (while transmitting this dummy seal blow-down force to the load cell). Thus for every pressure loading case (every curve in Figure 5), we have the force-displacement curve starting at a different negative force other than zero. However, since shifting these curves does not affect the stiffness value, we have zeroed out the starting force on each curve and presented these to start with the same zero force at 10 mils (0.254 mm) clearance.

Comparing the four curves in Figure 5, we see that the hysteresis in the test data (brush seal hysteresis + test rig hysteresis) increases with increasing pressure. The brush seal hysteresis portion of these test data is a result of inter-bristle friction forces and the friction between the bristles and the back plate. With increasing pressure loading, the normal reaction between the bristles and the back plate increases,

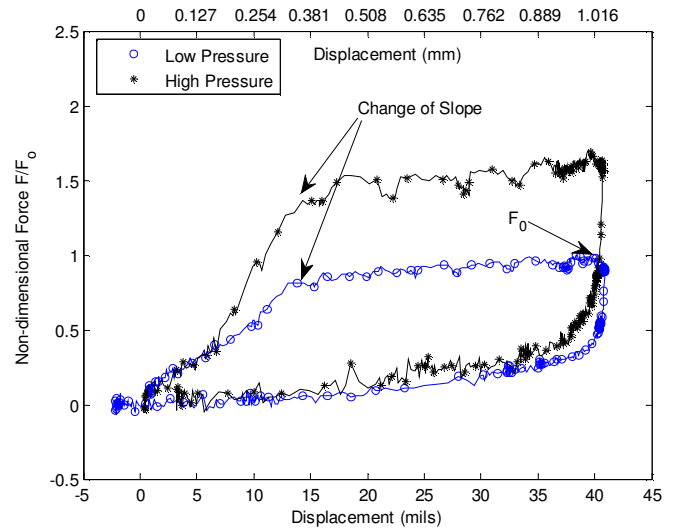


**Figure 6: Non-dimensional force-displacement plots for seal sample 3 at low and high pressure. The bi-linear nature of these curves is seen from the slope change around 15 mils interference. Unlike other test seals, these tests were performed starting with line-on-line assembly.**

thereby increasing the frictional resistance to bristle motion and causing brush seal hysteresis. Different back plate design features that reduce this friction force lead to different hysteresis behavior. The stiffness rig developed here indirectly (through load cell measurements) allows us to quantify the hysteresis behavior of different brush seal samples with different back plate designs.

From Figure 5, we also see that with increasing pressure, the slope of the force-displacement curves increases; indicating an increased stiffness with pressure. However, note that for sample seal 1 data presented in Figure 5, the increase in stiffness (i.e. slope) with increased pressure is not as dramatic (as compared to seal sample 2 with data shown in Figure 7 later). A remarkable feature of the force-displacement curves in Figure 5 for increasing displacements is that they are not perfectly linear. In other words, the slope of the force-displacement curve depends on the value of rotor displacement. For some tested seal samples, the force-displacement curves were found to be quite nonlinear, while for others, these curves were linear. It is also interesting to note that for some tested seal samples, we found the force-displacement curves to be bi-linear in nature. For these samples, as the rotor displacement is increased (for a given pressure loading), the force first increases rapidly (indicating a large stiffness) but increases gradually for high values of displacement. This bi-linear force-displacement behavior for seal sample 3 is shown in Figure 6. For test seals displaying such bi-linear force-displacement relationship, it is difficult to estimate a seal stiffness value. Further investigation is needed

to understand the bi-linear nature of these force-displacement curves, which point to the rapidly changing rotor-bristle force at small displacements (higher stiffness at small displacements) followed by relatively slowly changing rotor-bristle forces for larger rotor incursions. We point out that similar bi-linear behavior is also found in some test data presented in the work of Aksoy and Aksit [10].

Next we compare how seal stiffness changes with changing pressure loading. In this article, we present linear stiffness calculations only for seal sample 1 and seal sample 2 based on the assumption that the force-displacement relation is linear in the displacement range of 0 to 20 mils (seal sample 1) and 2 to 25 mils (seal sample 2). The linear stiffness values for different pressure loading cases for seal sample 1 and seal sample 2 are calculated using all data points between the above-mentioned limits and are shown in Figure 7. Stiffness data is not presented for seal sample 3 due to the bi-linear nature of the force-displacement curves shown in Figure 6. We point out that the stiffness values are non-dimensionalized by their respective zero-pressure loading stiffness values. As a consequence, both data sets start with non-dimensional stiffness 1 at zero pressure loading case. Also note that the stiffness values presented in Figure 7 are the average stiffness values estimated over 4 separate runs (repeats) for seal sample 1 and 3 separate runs (repeats) for seal sample 2. The uncertainty bars in Figure 7 are the maximum and minimum non-dimensional stiffness measured over the repeats for respective seal samples. The average uncertainty<sup>3</sup> is 28.18% for seal sample 1 and 30.01% for seal sample 2. For seal sample 2, the uncertainty is more or less same at low as well as high pressure loadings. For seal sample 1, the uncertainty increases with pressure loading.

As seen in Figure 7, seal sample 2 displays more pressure stiffening effect compared to seal sample 1. Clearly, seal sample 1 is a better choice for high-pressure applications where increased seal stiffness might cause seal wear and rotor dynamic instabilities. The stiffness rig developed in this article gives us a tool for investigating several such seal samples for their pressure stiffening effects. Furthermore, the test data shown in Figure 7 can be used to develop correlations or models for predicting pressure stiffening of brush seals.

## 5.0 CONCLUSIONS

Brush seals are widely used as a better alternative over labyrinth seals for sealing rotor-stator gaps in many turbo-machinery applications like steam turbines, gas turbines and aircraft engines. Pressure stiffening and hysteresis limit the usage of brush seals at high-pressure loading. In this article, we presented a non-rotating test rig for characterizing

<sup>3</sup> At every pressure loading we calculate percentage uncertainty as the difference between maximum and minimum stiffness divided by the average stiffness. We then calculate the average of these percentage uncertainty values over seven cases including the zero pressure case and the six pressure loaded cases to report an average uncertainty for the seal sample over all pressures.

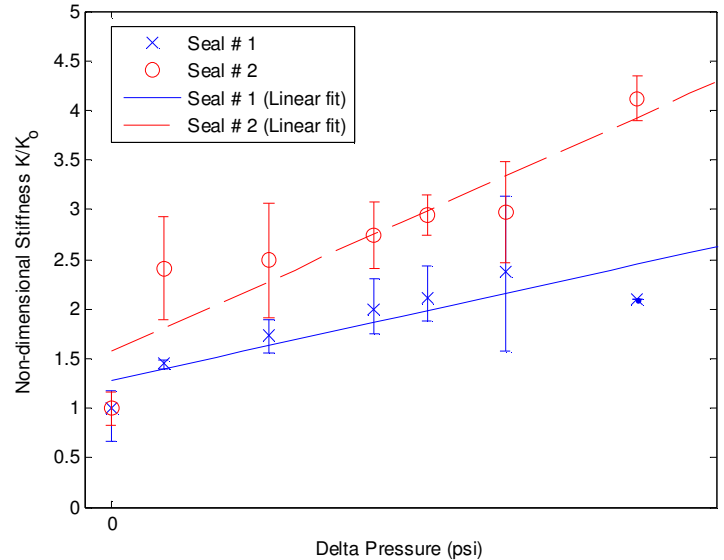


**Figure 7: Non-dimensional stiffness of seal sample 1 and seal sample 2 as a function of pressure loadings across the brush seal. The uncertainty bars represent the maximum and the minimum non-dimensional stiffness obtained over the repeat tests for the respective seals.**

large-diameter brush seals for their pressure-stiffening and hysteresis effects. The test rig's capabilities for differentiating between two pressure loading conditions for the same test seal, and ability to differentiate between two test seals for identical pressure loadings was demonstrated through representative test data. The test data presented here shows that the pressure stiffening and hysteresis depend on seal geometry and back plate designs.

## ACKNOWLEDGMENTS

We would like to thank Bernard Couture, Kim Clark, Michael Mack, William Adis, Binayak Roy, Deepak Trivedi, Ken Moore, Gene Palmer and James Graham of the General Electric Company for their help in this research. We are thankful to the anonymous reviewers for useful suggestions to improve the quality of this work and its presentation.

## REFERENCES

1. R.E. Chupp, F. Ghasripoor, N.A. Turnquist, M. Demiroglu & M.F. Aksit, 2002, "Advanced Seals for Industrial Applications: Dynamic Seal Development," *Journal of Propulsion and Power*, vol. 18(6), pp. 1260-1266.
2. S. Dinc, M. Demiroglu, N.A. Turnquist, J. Mortzheim, G. Goetze, J. Maupin, J. Hopkins, C. Wolfe & M. Florin, 2002, "Fundamental Design Issues of Brush Seals for Industrial Applications," *Trans. ASME - Journal of Turbomachinery*, vol. 124, pp. 293-300.

3. R.E. Chupp & C.A. Dowler, 1993, "Performance Characteristics of Brush Seals for Limited-Life Engines," *Trans. ASME- Journal of Engineering for Gas Turbines and Power*, vol. 115(2), pp. 390-397.
4. J.A. Carlile, R.C. Hendricks & D.A. Yoder, 1993, "Brush Seal Leakage Performance with Gaseous Working Fluids at static and Low Rotor Speed Conditions," *Trans. ASME- Journal of Engineering for Gas Turbines and Power*, vol. 115 (2), pp. 397-403
5. Y. Dogu & M. F. Aksit, 2006, "Effects of Geometry on Brush Seal Pressure and Flow Fields-- Part I: Front Plate Configurations," *Trans. ASME-Journal of Turbomachinery*, vol. 128 (2), pp. 367-378.
6. Y. Dogu & M. F. Aksit, 2006, "Effects of Geometry on Brush Seal Pressure and Flow Fields-- Part II: Backing Plate Configurations," *Trans. ASME-Journal of Turbomachinery*, vol. 128 (2), pp. 379-389.
7. W. Kellenberger, 1980, "Spiral Vibrations due to Seal rings in Turbogenerators: Thermally induced Interaction between Rotor and Stator," *Trans. of ASME - Journal of Mechanical Design*, vol. 102, pp. 177-184.
8. P. Goldman & A. Muszynska, 1995, "Rotor-to-stator, Rub-related, Thermal/Mechanical Effects in Rotating Machinery," *Chaos, Solitons & Fractals*, vol. 5 (9), pp. 1579-1601.
9. P. Basu, A. Datta, R. Loewenthal, J. Short & R. Johnson, 1994, "Hysteresis and Bristle Stiffening Effects in Brush Seals," *Journal of Propulsion and Power*, vol. 10 (4), pp. 569-575.
10. S. Aksoy & M. F. Aksit, 2010, "Evaluation of Pressure-Stiffness Coupling in Brush Seals," Paper No. *AIAA 2010-6831*, 46th AIAA/ASME/SAE/ASEE Joint Propulsion Conference & Exhibit, 25-28 July, Nashville, TN.
11. R. Flower, 1990, "Brush seal development system," 26th AIAA/SAE/ASME/ASEE Joint Propulsion Conference, Orlando, FL.
12. M. Demiroglu and J.A. Tichy, 2007, "An investigation of Tip Force characteristics of brush seals," Paper No: GT2007-28042, ASME Turbo Expo Power, Land and Air, May 14-17, Montreal Canada.
13. P. F. Crudginton & A. Bowsher, 2002, "Brush Seal Pack Hysteresis," 38th AIAA/ASME/SAE/ASEE Joint Propulsion Conference & Exhibit, 7-10 July, Indianapolis, IN.
14. P. E. Wood & T. V. Jones, 1999, "A Test Facility for the Measurement of Torques at the Shaft to Seal Interface in Brush Seals," *Trans. ASME- Journal of Engineering for Gas Turbines and Power*, vol. 121, pp. 160-166.
15. H. Zhao & R. Stango, 2005, "An analytical approach for investigating bristle/backplate hysteresis phenomenon in brush seals," Paper No. *AIAA 2005-3983*, 41st AIAA/ASME/SAE/ASEE Joint Propulsion Conference & Exhibit, 10-13 July, Tucson, AZ.